

TREATMENT OF SPECTRAL EFFECTS IN PARTICIPATING MEDIA RADIATION MODELING

Anderson Mossi, mossi@uffs.edu.br

Federal University of Fronteira Sul, Av. Sete de Setembro 1305 – Erechim – RS

Vinayak Barve, vinayakbarve@gmail.com

Siemens, Orlando, FL – USA

Marcelo Galarça, marcelo.galarca@riogrande.ifrs.edu.br

Federal Institute of Rio Grande do Sul, Rua Eng. Alfredo Huch, 475 - Rio Grande - RS

Horacio Vielmo, vielmoh@mecanica.ufrgs.br

Francis França, frfranca@mecanica.ufrgs.br

Federal University of Rio Grande do Sul, Sarmento Leite, 425 – Porto Alegre – RS

Ofodike Ezekoye, dezekoye@mail.utexas.edu

University of Texas at Austin, University Station – Austin – TX – USA

Abstract. *Good prediction in the divergence of the radiative heat flux is demanded in combustion problem simulations, because both the high temperatures and gases formation involved in the process make the radiation be the most important heat transfer mode. To obtain the divergence of the radiative heat flux is necessary an integration of the radiative transfer equation (RTE) in all directions and all spectral lines, but even nowadays these calculations are extremely time consuming, so it is necessary the use of gas models to obtain solutions in a reasonable time. In this work, it is used a finite volume code to simulate a steady methane-air diffusion flame. This code solves the equations for the conservation of mass, momentum, individual species, and energy. It also has a soot chemistry model and a discrete ordinates radiation model, where the gas absorption coefficient is modeled in two different ways: the oversimplified gray gas model and the spectral line based on the weighted sum of grays gases (SLW) model. The results for the temperature distribution, gas species concentration, and soot formation are confronted with the two different radiation gas models used. The overall differences of the results for the different gas models and the computational cost of the simulations are detailed.*

Keywords: *Radiation Heat Transfer, Spectral Models, Combustion, Diffusion Flames*

1. INTRODUCTION

This work analyses the effects of thermal radiation heat transfer in diffusion flames. In these kinds of flame, fuel and oxidizer are initially separated and combustion is diffusion controlled. Since Combustion problems involve a number of coupled phenomena, such as chemical kinetics, fluid flow, soot production, heat transfer, etc. An accurate prediction of the thermal radiation heat transfer in participating gases, which is a heat transfer mechanism in combustion, is necessary to get appropriate solutions for this complex phenomenon. On the other hand, its modeling is difficult due to the highly complex dependence of the absorption coefficient with the wavelength, which can be characterized by hundreds of thousands spectral lines. Thus, the solution of the radiative heat transfer equation is very expensive or even impossible without modeling the gas absorption coefficient. The radiative transfer equation is frequently solved with the gray gas assumption, where the dependence of the absorption coefficient over the wavelength is neglected. Between the spectral dependence models, the weighted-sum-of-gray-gases (WSGG), developed by Hottel and Sarofim (1967) is another method widely used nowadays. It models the entire spectrum by a few bands having uniform absorption coefficients, where each band corresponding to a gray gas. The weighting coefficients account the contribution of each gray gas corresponding to the fractions of the blackbody energy in the spectrum region where the gray gases are located. In general, those coefficients are obtained from fitting experimental data, such as those presented in Smith et al. (1982) and Smith et al. (1987). The spectral-line based on the weighted-sum-of-gray-gases (SLW) method (Denison and Webb, (1993)) is based on the same WSGG equation, but differs in the calculations of the absorption coefficient and in the weights as well. In this model, the spectrum is divided in n supplemental absorption cross-sections, and then the absorption coefficient is considered gray between two adjacent ones. Their weights are defined by the difference of the absorption line blackbody (ALB) distribution function measured at those adjacent supplemental absorption cross-sections. Thus, the same RTE proposed by Modest (1991) for the WSGG model is solved. The full spectrum correlated-k distribution (FSK) method (Moedst and Zhang (2002)) also uses the WSGG equation and the ALB distribution function. In this method, the absorption coefficient is a function obtained from the inversion of the ALB distribution function calculated in the local thermodynamic state, and the weights are calculated by the derivative of the ALB distribution function evaluated in the local thermodynamic state over the one calculated in a reference state.

The cumulative wavenumber (CW) method (Solovjov and Webb, (2002)), uses the cumulative wavenumber function to describe the dependence of the absorption coefficient over the wavenumber, but this method is very expensive even for two-dimensional problems. Due to this problem, the fast approximate technique for the CW method (Salinas, 2008), which reduces one constraint in radiative transfer equation, can be applied in multi-dimension problems to get faster results. Recently, Solovjov and Webb (2010) proposed the SLW-CW approach that uses both the CW function and the ALB distribution function to solve the RTE. This method is faster than CW, but needs two spectral functions: one for the cumulative wavenumber and another one for the ALB distribution function.

In this work, a diffusion flame in a cylindrical geometry is solved, taking account the soot production, the chemical reactions of the methane with air, and the radiative divergence of the heat flux is calculated, where the RTE is solved with the discrete ordinates method and the absorption coefficient of the gases is modeled with two different approaches: the gray gas model and the SLW model.

2. NUMERICAL SIMULATIONS

A finite volume CFDC (Computational Fluid Dynamics with Chemistry) code – UNICORN (Katta et al. 1994) is used in this study for simulating the CH₄-air diffusion flames. UNICORN (UNsteady Ignition and COmbustion with ReactionNs) solves the equations for the conservation of mass, momentum, individual species and energy in the unsteady formulation. It also has a soot chemistry model and a DOM radiation model. The cylindrical form of the conservation equations is solved on a 2D axisymmetric staggered grid.

2.1. The Conservation of Mass Equation

The continuity equation is used to resolve the velocities due to the pressure gradients. The continuity equation in cylindrical coordinates is given as:

$$\frac{\partial \rho}{\partial t} + \frac{1}{r} \frac{\partial(\rho r v)}{\partial r} + \frac{\partial(\rho u)}{\partial z} = 0 \quad (1)$$

2.2. The Conservation of Momentum Equation

The axial momentum equation in cylindrical coordinates can be written as

$$\begin{aligned} \frac{\partial(\rho u)}{\partial t} + \frac{\partial(\rho u u)}{\partial z} + \frac{\partial(\rho v u)}{\partial r} = \frac{\partial}{\partial z} \left(\mu \frac{\partial u}{\partial z} \right) + \frac{\partial}{\partial r} \left(\mu \frac{\partial u}{\partial r} \right) - \frac{\rho v u}{r} + \frac{\mu}{r} \frac{\partial u}{\partial r} - \frac{\partial P}{\partial z} + (\rho_o - \rho)g + \frac{\partial}{\partial z} \left(\mu \frac{\partial u}{\partial z} \right) + \frac{\partial}{\partial r} \left(\mu \frac{\partial v}{\partial z} \right) + \\ \frac{\mu}{r} \frac{\partial v}{\partial z} - \frac{2}{3} \left[\frac{\partial}{\partial z} \left(\mu \frac{\partial u}{\partial z} \right) + \frac{\partial}{\partial z} \left(\mu \frac{\partial v}{\partial r} \right) + \frac{\partial}{\partial z} \left(\mu \frac{v}{r} \right) \right] \end{aligned} \quad (2)$$

and the radial momentum equation is given as

$$\begin{aligned} \frac{\partial(\rho v)}{\partial t} + \frac{\partial(\rho u v)}{\partial z} + \frac{\partial(\rho v v)}{\partial r} = \frac{\partial}{\partial z} \left(\mu \frac{\partial v}{\partial z} \right) + \frac{\partial}{\partial r} \left(\mu \frac{\partial v}{\partial r} \right) - \frac{\rho v v}{r} + \frac{\mu}{r} \frac{\partial v}{\partial r} - \frac{\partial P}{\partial r} + \frac{\partial}{\partial z} \left(\mu \frac{\partial u}{\partial r} \right) + \frac{\partial}{\partial r} \left(\mu \frac{\partial v}{\partial r} \right) + \frac{\mu}{r} \frac{\partial v}{\partial z} - \\ 2\mu \frac{v}{r^2} - \frac{2}{3} \left[\frac{\partial}{\partial r} \left(\mu \frac{\partial u}{\partial z} \right) + \frac{\partial}{\partial r} \left(\mu \frac{\partial v}{\partial r} \right) + \frac{\partial}{\partial r} \left(\mu \frac{v}{r} \right) \right] \end{aligned} \quad (3)$$

The pressure-projection method (Peyret and Taylor, 1983) is used to couple the pressure with the velocity. This method involves splitting the momentum equation into two parts, where the first part handles the effects of the convective, body parts and viscous terms, and the second part handles the effects of the pressure gradient.

2.3. Conservation of Species Equation

The conservation of species equation is solved for all the species but CO₂. In cylindrical coordinates, it is written as:

$$\frac{\partial(\rho Y_i)}{\partial t} + \frac{1}{r} \frac{\partial(\rho r v Y_i)}{\partial r} + \frac{\partial(\rho u Y_i)}{\partial z} = \frac{1}{r} \frac{\partial}{\partial r} \left(\rho r D \frac{\partial Y_i}{\partial r} \right) + \frac{\partial}{\partial z} \left(\rho D \frac{\partial Y_i}{\partial z} \right) + \dot{r} \quad (4)$$

where \dot{r} is the rate of generation or depletion of the species. The convection-diffusion effects in the species equation are resolved using the hybrid method as suggested by Patankar (1980). The scheme examines the Peclet number

($Pe=u\Delta x/D$) for each cell. The Peclet number is the ratio of the convective component due to the velocity, and the diffusion component. If the magnitude of the cell Peclet Number is greater than or equal to 2, the diffusion effects are neglected in the discretization and only the convection effects are used. This results in an upwind scheme. On the other hand, if the magnitude of the cell Peclet number is less than 2, both the diffusion and convection effects are considered. For discretizing the diffusion effects, central difference schemes are used.

The source or sink term \dot{r} is calculated based on the species concentrations and the finite rate reaction rates. The model used here is essentially the chemistry mechanism used by Peters (1993) with the rates for 6 reactions modified for ease of calculation and due to the corrections recommended by Katta et al. (1998). The mechanism uses 30 species and 101 reaction rates. The species solved are CH₄, CH₃, CH₂, CH, CH₂O, CHO, CO₂, CO, H₂, H, O, OH, H₂O, HO₂, H₂O, C₂H, C₂H₂, C₂H₃, C₂H₄, C₂H₅, C₂H₆, CHCO, C₃H₃, C₃H₄, C₃H₅, C₃H₆, nC₃H₇, iC₃H₇, O₂ and N₂.

2.4. Soot Chemistry

A simplified two-equation soot model (Leung et al. (1991) and Fairweather et al. (1992)) is added to the chemistry mechanism for modeling soot. The two equations solved are the equations for conservation of the soot mass fraction and the soot number density. The soot chemistry is modeled by accounting for soot formation and surface growth from acetylene (C₂H₂) only. The corresponding equations are as:

$$\frac{\partial(\rho Y_s)}{\partial t} + (v + v_{th}) \frac{\partial(\rho Y_s)}{\partial r} + (u + u_{th}) \frac{\partial(\rho Y_s)}{\partial z} = \dot{r} \quad (5)$$

$$\frac{\partial(\rho N_s)}{\partial t} + (v + v_{th}) \frac{\partial(\rho N_s)}{\partial r} + (u + u_{th}) \frac{\partial(\rho N_s)}{\partial z} = \dot{r}_N \quad (6)$$

In the above equations, the diffusive terms from the species conservation equation are neglected since the $Sc \gg 1$ (Ezekoye and Zhang, 1997). The thermophoretic velocities are calculated as

$$u_{th} = -0.55 \frac{\mu}{\rho T} \frac{dT}{dx} \quad (7)$$

and

$$v_{th} = -0.55 \frac{\mu}{\rho T} \frac{dT}{dr} \quad (8)$$

where \dot{r} is the source or sink term for the soot mass fraction and \dot{r}_N is the corresponding term for the soot number density.

Table 1: Reaction Mechanism for the soot chemistry.

No	Reaction	A	N	Ea
102	$C_2H_2 \Rightarrow 2C(s) + H_2$	1.35E6	0	41000
103	$C_2H_2 + nC(s) \Rightarrow (n + 2)C(s) + H_2$	5E2	0	24000
104	$C(s) + \frac{1}{2}O_2 \Rightarrow CO$	1.78E4	0.5	39000
105	$C(s) + OH \Rightarrow CO + H$	1.06E2	-0.5	0
106	$C(s) + O \Rightarrow CO$	5.54E10	-0.5	0

The soot species reaction mechanism has soot nucleation, surface growth and oxidation, while the number particle mechanism accounts for the soot nucleation and agglomeration. Table 1 lists the reaction mechanism and the corresponding reaction rates for the soot model. Reaction 1 is the nucleation reaction while reaction 2 is the surface growth reaction. Reactions 3, 4 and 5 are the soot oxidation steps due to O₂, OH and O respectively. In this study, we have applied the approach of Guo et al (2002) and included soot oxidation from O₂, OH and O. The soot mass fraction reaction rate term (\dot{r}) is calculated based on the reactions given in Tab.1 as:

$$\dot{r} = M_{C(s)} (\omega_{102} + \omega_{103} - \omega_{104} - \omega_{105} - \omega_{106}) \quad (9)$$

where,

$$\omega_{102} = k_{102}(T)[C_2H_2] \quad (10)$$

$$\omega_{103} = k_{103}(T)A_s[C_2H_2] \quad (11)$$

$$\omega_{104} = k_{104}(T)[O_2]A_s \quad (12)$$

$$\omega_{105} = \phi_{OH}k_{105}(T)X_{OH}A_s \quad (13)$$

$M_{C(s)}$ is the molecular weight of carbon or soot ($M_{C(s)} = 12.011$ kg/kmol) and A_s is the soot surface area per unit volume and is calculated as:

$$A_s = \pi d_p^2 \rho N = \pi \left(\frac{6}{\pi} \frac{1}{\rho_s} \frac{Y_s}{N} \right)^{2/3} (\rho N) \quad (14)$$

In this model, soot surface growth varies linearly with the soot surface area per unit volume. ϕ_O is the collision efficiency of the O attack on soot particles and its value is taken as 0.5. ϕ_{OH} stands for the collision efficiency of the OH attack on soot particles. ϕ_{OH} is calculated using the method suggested by Kennedy et al. (1996). They accounted for the variation in the collision efficiency with residence time of the soot particle by varying the value of ϕ_{OH} based on the distance from the fuel nozzle edge. The value is varied linearly from 0.05 to 0.2 as a function of the normalized downstream distance (x/D). For distances beyond x/D of 7, value of 0.2 was used. In the present study, since the internal nozzle is simulated, a value of 0.05 was used within the nozzle for ϕ_{OH} .

The source term in the soot particle number concentration equation is calculated as:

$$\dot{r}_N = \frac{2}{C_{\min}} N_A \omega_1 - 2C_a \left(\frac{6M_{C(s)}}{\pi \rho_{C(s)}} \right)^{1/6} \left(\frac{6\kappa T}{\rho_{C(s)}} \right)^{1/2} [C(s)]^{1/6} [\rho N]^{11/6} \quad (15)$$

The first term on the right represents the nucleation term for the particle number equation, while the second term accounts for particle agglomeration. N_A is Avogadro's number (6.022×10^{26} particles/kmol), C_{\min} is the number of carbon atoms in the incipient carbon molecule (9×10^4), κ is the Boltzmann constant (1.38×10^{-23} J/K), C_a is the agglomeration rate constant (3.0) and $\rho_{C(s)}$ is the density of the soot particle (2000 kg/m³).

2.5. The Energy Equation

Once the species concentrations are known at each grid point, the total enthalpy form of the conservation of energy equation is solved in an implicit formulation, and it includes the enthalpy of formation of the species. The total enthalpy for each species is a function of temperature. Polynomial curve fits of the enthalpy data have been obtained based on the JANAF data, 1998. These expressions are used to calculate the total enthalpy H and the specific heats (c_p) for each species at each grid point.

The total enthalpy equation has the form:

$$\frac{\partial(\rho H)}{\partial t} + \nabla \cdot \rho H \vec{V} = \nabla \cdot \left(\frac{k}{c_p} \nabla H - q_r \right) + \nabla \cdot \sum_i H_i \left(-\frac{k}{c_p} + \rho D_i \right) \nabla \sum_i \frac{Y_i}{M_i} \quad (16)$$

where,

$$H = \sum_i \frac{H_i Y_i}{M_i} \quad (17)$$

and

$$c_p = \sum_i \frac{c_{pi} Y_i}{M_i} \quad (18)$$

where i is the species index. The convection-diffusion balance is resolved in the same way (hybrid scheme) as the species equations. In this case, when the cell Peclet number (based on the thermal diffusivity) is greater than 2, the first term on the right hand side is neglected. $\nabla \cdot q_r$ is the divergence of the radiative heat flux vector and this term continues to be resolved irrespective of the cell Peclet number. The second term on the right hand side resolves the differential diffusion effects.

Once the total enthalpy at each grid point is known, the cell temperatures can be calculated. Based on the already calculated species mass fractions and the total enthalpy at each cell, the cell temperature is calculated by first assuming the temperature range i.e. ≤ 1000 K or ≥ 1000 K. Then, an initial guess of 1000 K for $T \leq 1000$ K range or a guess of 5000 K for $T \geq 1000$ K range is made. The temperatures are then adjusted by using a step ΔT calculated from the thermodynamic expression, $d\hat{H} = c_p dT$. This gives,

$$\Delta T = T_{\text{guess}} - T_{\text{new}} = \frac{H - H(T_{\text{guess}})}{c_p(T_{\text{guess}})} \quad (19)$$

Temperatures are adjusted in an iterative manner until the difference in the new and guess temperature is less than 0.001 K.

The enthalpy and specific heats for soot have been calculated as functions of the local temperature by using polynomial fits based on the temperature on the data available from the Chase (1998). For soot, data from the 'carbon' listings in Chase (1998) was used.

2.6. Radiation Heat Transfer

The radiative transfer equation for non-scattering media, in cylindrical coordinates, with the discrete ordinates method, is given by:

$$\frac{\partial I_\eta}{\partial s} = \mu \frac{\partial I_\eta}{\partial r} + \xi \frac{\partial I_\eta}{\partial z} - \frac{\zeta}{r} \frac{\partial I_\eta}{\partial \varphi} = -\kappa_\eta I_\eta + \kappa_\eta I_{b\eta} \quad (20)$$

subject to

$$I_{\eta w} = \varepsilon_{\eta w} I_{b\eta}(T_w) + \frac{(1 - \varepsilon_{\eta w})}{\pi} \int_{\hat{n} \cdot \hat{s}} I_\eta |\hat{n} \cdot \hat{s}| d\Omega \quad (21)$$

where μ , ζ , and ξ are the directions, η is the wavenumber, $I_{b\eta}$ is the blackbody intensity, I_η is the intensity, and κ_η is the absorption coefficient, given by:

$$\kappa_\eta = N \sum_i \frac{S_i}{\pi} \frac{\gamma_i}{(\eta - \eta_i)^2 + \gamma_i^2} \quad (22)$$

where S_i [$\text{cm}^{-1}/(\text{molecule} \times \text{cm}^2)$] is the integrated line intensity, η_i [cm^{-1}] is the line location, and γ_i [$\text{cm}^{-1}/\text{atm}$] is the half-width, which is a function of the mole fraction Y_s , described by:

$$\gamma_i = \left(\frac{T_{ref}}{T}\right)^n Y_s \gamma_{self,i} + \left(\frac{T_{ref}}{T}\right)^{0.5} (1 - Y_s) \gamma_{air,i} \quad (23)$$

where T is the temperature, γ_{self} and γ_{air} are the self broadening half-width and air broadening half-width, respectively, and n is the temperature dependent coefficient. The values of η_i , S_i , γ_{self} , γ_{air} and n can be obtained either from HITRAN or HITEMP, among other databases.

Once the RTE is solved, the divergence of the radiative heat flux, presented in the energy equation, is calculated as:

$$\nabla \cdot q = \int_{\Omega} \int_{\eta} (-\kappa_\eta I_\eta + \kappa_\eta I_{b\eta}) d\eta d\Omega \quad (24)$$

Solving Eq. (20) for every single absorption coefficient value is almost impossible, because the absorption coefficient is strongly dependent on wavenumber. Due to this fact, gas models have been used to solve the RTE quickly. A brief description of the gas models used in this work is described below.

2.6.1. Gray Gas Model

Many researchers, especially to solve 3D problems, have used the assumption that the gas is gray. The RTE for non-scattering media, with the gray gas model, becomes:

$$\frac{dI}{ds} = -\kappa I + \kappa I_b \quad (25)$$

with boundary conditions defined as:

$$I_w = \varepsilon_w I_b(T_w) + \frac{(1-\varepsilon_w)}{\pi} \int_{\hat{n} \cdot \hat{s}} I |\hat{n} \cdot \hat{s}| d\Omega \quad (26)$$

Table 2: Curve fits for the absorption coefficient used in the gray gas model

Species	Absorption Coefficients	
CO	$\kappa = c_0 + T(c_1 + T(c_2 + T(c_3 + Tc_4)))$ in $\text{m}^{-1}\text{atm}^{-1}$	
		$300 \leq T \leq 750$ $750 < T \leq 2500$
	c_0	4.7869 10.09
	c_1	-0.06953 -0.01183
	c_2	2.95775×10^{-4} 4.7753×10^{-6}
	c_3	-4.25732×10^{-7} -5.87209×10^{-10}
	c_4	2.02894×10^{-10} -2.5334×10^{-14}
CO ₂ and H ₂ O	$\kappa = \sum_{i=0}^5 c_i (1000/T)^i$ in $\text{m}^{-1}\text{atm}^{-1}$	
		H ₂ O CO ₂
	c_0	-0.23093 18.741
	c_1	1.1239 -121.31
	c_2	9.4153 273.5
	c_3	-2.9988 -194.05
	c_4	0.51382 56.31
c_5	-1.8684×10^{-5} -5.8169	
C	$\kappa = 1186f_s T$ in m^{-1}	

In this work, the absorption coefficients for CO, CO₂, and H₂O are correlated by Barlow et al. (2001) and the absorption coefficient for the soot is calculated as suggested by Atreya et al. (1998). These curve fits are listed in Tab 2.

2.6.2. The Spectral Line Based Weighted-Sum-of-Gray-Gases Model (SLW)

In this model, the gas absorption cross-section (C_η) range is divided into n gray gases. For each gray gas, the RTE, given in Eq. (20) is integrated over all intervals $\Delta\eta_i$, where the gas absorption cross-section is less than the gray gas value (C_j), according to Eq (27).

$$\sum_i \int_{\Delta\eta_{i,j}} \frac{dI_\eta}{ds} d\eta = \sum_i \int_{\Delta\eta_{i,j}} (-\kappa_\eta I_\eta + \kappa_\eta I_{b\eta}) d\eta \quad (27)$$

Applying the Leibniz integral rule in the left hand side term of Eq. (27), and assuming that κ_η is constant inside the interval $\Delta\eta_i$, we have:

$$\frac{d}{ds} \left[\sum_i \int_{\Delta\eta_{i,j}} I_\eta d\eta \right] = -\kappa_j \sum_i \int_{\Delta\eta_{i,j}} I_\eta d\eta + \kappa_j \sum_i \int_{\Delta\eta_{i,j}} I_{b\eta} d\eta + \sum_i I_\eta(\eta_{i,j}^u) \frac{d\eta_{i,j}^u}{ds} - \sum_i I_\eta(\eta_{i,j}^l) \frac{d\eta_{i,j}^l}{ds} \quad (28)$$

where the superscripts l and u represents the lower and upper limits of the i th spectral interval, respectively. Finally, neglecting the two last terms of Eq. (28), generated by the Leibniz integral rule, the RTE for the SLW model is:

$$\frac{\partial I_j}{\partial s} = -\kappa_j I_j + \kappa_j a_j I_b \quad (29)$$

where

$$I_j = \sum_i \int_{\Delta\eta_{i,j}} I_\eta d\eta \quad (30)$$

in this model, I_j is viewed as the integrated intensity, κ_j is the absorption coefficient, and a_j is the corresponding blackbody weight, all associated with the j th gray gas.

In the SLW model, the absorption coefficients are considered gray between two adjacent gray gases. The weights associated with the fraction of the radiative blackbody energy are calculated in those parts where the absorption cross-section C_η is less than the gray gas C is defined by the ALB distribution function as:

$$F(C) = \frac{1}{\sigma T_b^4} \int_{\{C_\eta \leq C\}} E_{b\eta}(T_b, \eta) d\eta \quad (31)$$

where $E_{b\eta}(T_b, \eta)$ is the Planck blackbody energy function, and T_b is the source temperature, as defined by Atreya et al. (1998). Then, in the SLW model, the weights are calculated as a difference between two adjacent values of the ALB distribution function, according to Eq. (32).

$$a_j = F(C_j) - F(C_{j-1}) \quad (32)$$

and the absorption coefficient is obtained as:

$$\kappa_j = N \sqrt{C_j C_{j-1}} \quad (33)$$

where N is the molar density.

Applying the SLW model to gas mixtures is hard, because the ALB distribution function must be calculated for every concentration in every single temperature. To make it easier, Solovjov and Webb (2000) presented some useful approaches.

For different concentrations, if the air self-broadening were neglected, the following relation is valid for the ALB distribution function:

$$F_{YC_\eta}(C) = F_{C_\eta}(C/Y) \quad (34)$$

This relation is very useful when the problem has non-uniform spatial concentration distribution. For a mixture of gases, it was used the multiplication approach, defined by:

$$F(C_j) = \prod_{i=1}^m F_j(C_j/Y_i) \quad (35)$$

3. RESULTS AND DISCUSSIONS

The simulations of a steady CH₄-air diffusion flame are performed considering a bi-dimensional cylindrical axisymmetric geometry with 10 cm of radius and 30 cm of axial length, as shown in Fig. 1.

The fuel tube radius is 0.5 cm and the air annulus radius is 5 cm. The internal part of the fuel nozzle was modeled with a length of 2 cm and a thickness of 0.05 cm. It was maintained at 550 K to model some of the fuel preheat effects due to a warm nozzle. The fuel stream and the air co-flow velocities were both at 7.9 cm/s and were maintained at 300 K. Symmetry boundary conditions were applied in the center line and zero gradient boundary conditions in the side wall. In the topside, non-reflecting boundary conditions were applied. A non-uniform grid with 281 volumes in the axial

direction and 121 volumes in the radial direction was used. The smallest grid spacing was applied near the nozzle exit and was stretched both in the axial and in the radial directions.

The simulations were performed in parallel, using 8 processors using the Lonestar cluster at the Texas Advanced Computing Center (TACC). Running the code with the gray gas model, it takes about 26 hours of simulation, while with the SLW model, the time increased to 48 hours. Comparisons were made to verify how the radiative heat transfer affects in the temperature field, in the H₂O, CO₂ and CO mole fractions, and in the soot formation, for the two different gas models used.

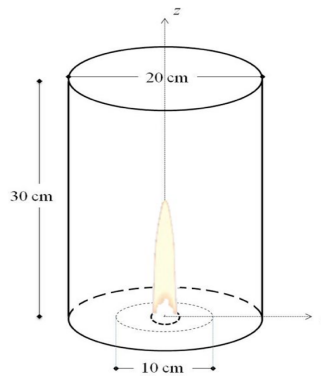


Figure 1: Schematic of the domain.

Figure 2 shows the results for the Temperature, H₂O and CO₂ mole fractions. the left hand side of Fig. 2a represents the temperature field obtained with the gray gas radiation model, and the right hand side represents the difference between the gray gas model and the SLW model, according to the following relation:

$$\% \text{ error} = 100 * \frac{(R_{GG} - R_{SLW})}{|R_{GG,max}|} \quad (36)$$

where R means the result that is being considered.

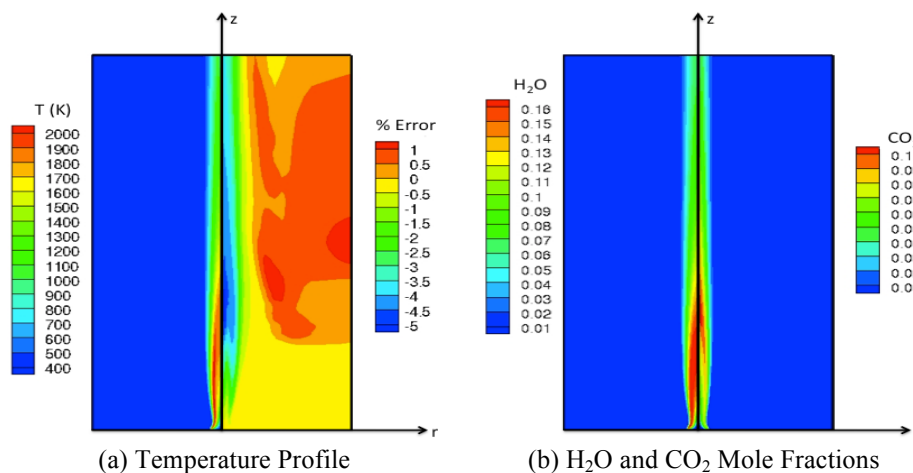


Figure 2: Temperature Field, H₂O and CO₂ mole fraction distributions.

As can be seen in Fig. 2a, the different radiation predictions affects directly in the temperature field. In this case, it is responsible for differences up to 130 K in the same problem. When the temperature changes, the activation energy changes too, so it affects directly in the formation and destruction of the species involved in the process. Figure 2b shows the H₂O and CO₂ mole fractions. These quantities do not vary significantly with the different radiation models, because they are primary substances, so they are practically independent of the temperature field. The variation of these substances using the different radiation models is less than 2% for both cases.

But the same issue does not happen with the CO distribution, as can be seen in Fig. 3a. The CO formation is more dependent on the temperature than the H₂O and CO₂, because its formation generally occurs when the temperature is bigger than 1500 K, then the variation in the temperature filed has an important role in those differences.

Preliminary results, not shown here, point that the SLW model does not account the soot correctly, and it could be responsible for the differences in the soot production shown in Fig. 3b. In this problem, the radiation from soot is so important as the one from the gases, then that difference up to 15% in the production (Fig. 3b), is the main reason for that difference in the temperature field (Fig. 2a). As can be seen in Fig. 4b, in the same region where the difference in the soot production is around 12%, the temperature field has its maximum deviation.

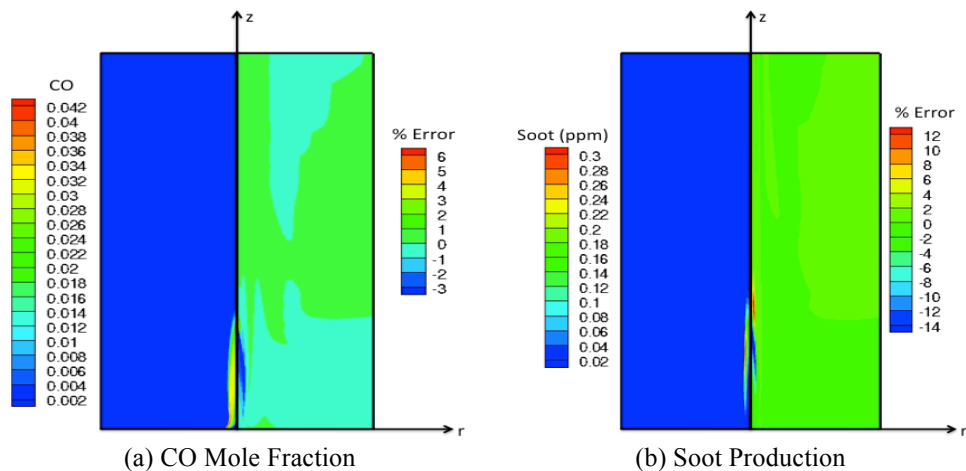


Figure 3: CO mole fraction and Soot distributions.

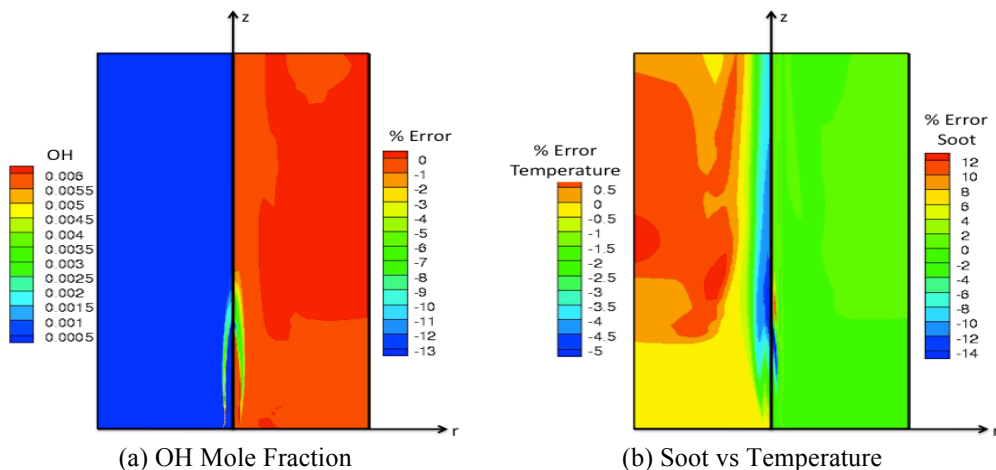


Figure 4: OH mole Fraction and a comparison between Soot and Temperature.

Figure 4a shows that the OH production and its difference between the radiation models are also significant, since the OH destroys the soot. This amount is also sensible to the temperature field and it is also responsible for the differences shown in Fig. 4b. That difference around -13% in the right hand side of Fig. 4a is correlated to the difference around 12% in the right hand-side of Fig. 4b, because the soot has been destroyed in that location.

4. CONCLUSIONS

This work showed the importance of a good prediction in the radiative heat transfer for combustion problems. Two different gas models were used: the gray gas and the SLW model. The comparison of the results obtained with these two models, showed that important amounts like soot, CO and OH are very sensible, and they also affected in the temperature field as well. Since the soot production changed significantly with the two radiation models used, it shows that to get correctly approaches for the soot, is mandatory the use a good radiation model in the simulations. But due the complexity of the combustion process, it is not trivial to attribute all these differences in the soot production and other species formation just to the radiation, but it is clear that it is a very important issue and cannot be undertreated in combustion predictions.

5. ACKNOWLEDGEMENTS

The authors thank CAPES (Brazil) for the support under the Program CAPES/UT-AUSTIN, No. 28/2008, and they also acknowledge the Texas Advanced Computing Center (TACC) at The University of Texas at Austin for providing computational and storage resources that have contributed to the research results reported within this paper. The first and second authors acknowledge the CNPq (Brazil) for the doctoral fellowship.

6. REFERENCES

- Atreya, A., Agrawal, S., 1998, "Effect of Radiative Heat Loss on Diffusion Flames in Quiescent Microgravity Atmosphere", *Combustion and Flame*, 115, pp 372-382.
- Barlow, R. S., Karpetis, A. N., Frank, J. H., 2001. "Scalar Profiles and NO Formation in Laminar Opposed-Flow Partially Premixed Methane/Air Flames", *Combustion and Flame*, 127, pp. 2102-2118.
- Chase, M.W., Jr., 1998. "NIST-JANAF Thermochemical Tables", Fourth Edition, *Journal of Physical and Chemical Reference Data*, Monograph 9, p 1-1951.
- Denison, M. K., Webb, B. W., 1993, "An Absorption-Line Blackbody Distribution Function for Efficient Calculation of Total Gas Radiative Transfer", *JQSRT*, 50, pp. 499-510.
- Ezekoye O.A. and Zhang, Z., 1997. "Soot Oxidation and Agglomeration Modeling in a Microgravity Diffusion Flame", *Combustion and Flame*, v 110, p 127-139.
- Fairweather, M., Jones, W.P. and Lindstedt, R.P., 1992. "Predictions of Radiative Transfer from a Turbulent Reacting Jet in a Cross-Wind", *Combustion and Flame*, v 89, p 45-63.
- Guo, H., Liu, F., Smallwood, G.J. and Gülder, Ö.L., 2002. "The Flame Preheating Effect on Numerical Modelling of Soot Formation in a Two-Dimensional Laminar Ethylene-Air Diffusion Flame", *Combustion Theory and Modelling*, v 6, p 173- 187.
- Hottel, H. C., Sarofim, A. F., 1967, "Radiative Transfer", McGraw-Hill Book Company.
- Katta, V.R., Goss L.P. and Roquemore, W.M., 1994. "Numerical Investigations of Transitional H₂/N₂ Jet Diffusion Flames", *AIAA Journal*, v 32, n 1, p 84.
- Katta, V.R., Hsu, K.Y. and Roquemore, W.M., 1998. "Local Extinction in an Unsteady Methane Air Jet Diffusion Flame", *Twenty-Seventh Symposium on Combustion*, The Combustion Institute, Pittsburgh, PA, p 1121-1129.
- Kennedy, I.M., Yam, C., Rapp, D.C. and Santoro, R.J., 1996. "Modeling and Measurements of Soot and Species in a Laminar Diffusion Flame", *Combustion and Flame*, v 107, p 368-382.
- Leung, K.M., Lindstedt, R.P. and Jones, W.P., 1991. "A Simplified Reaction Mechanism for Soot Formation in Nonpremixed Flames", *Combustion and Flame*, v 87, p 289- 305.
- Modest, M. F., 1991, "The Weighted-Sum-of-Gray-Gases Model for Arbitrary Solution Methods in Radiative Transfer", *J. Heat Transfer*, 113, pp.650-656.
- Modest, M. F., Zhang H., 2002, "The Full-Spectrum Correlated-k Distribution for Thermal Radiation from Molecular Gas-particulates Mixtures", *J. Heat Transfer*, 124, pp. 30-38.
- NIST-JANAF Thermochemical Tables 2 Volume-Set, 1998. "Journal of Physical and Chemical Reference Data Monographs", American Inst. of Physics. 4th edition.
- Patankar, S., 1980. "Numerical Heat Transfer and Fluid Flow", Taylor & Francis, 1st edition.
- Peters, N., 1993. "Reduced Kinetic Mechanisms for Applications in combustion systems, Lecture Notes in Physics", Springer-Verlag, Berlin, p314.
- Peyret, R., Taylor, T. 1983, "Computational methods for fluid flow", Springer Series in Computational Physics, Springer-Verlag, New York, 1983
- Rothman, L. S., 2009, "The HITRAN 2008 Molecular Database" *JQSRT*, 110, pp. 533-572.
- Rothman, L. S., Camy-Peyret, C., Flaud, J.-M., Gamache, R. R., Goldman, A., Goorvitch, D., Hawkins, R. L., Schroeder, J., Selby, J. E. A., and Wattson, R. B., 2002, "HITEMP, the High-Temperature Molecular Spectroscopic Database" *JQSRT*.
- Salinas, C. T., 2008, "Fast Approximate Technique for the Cumulative Wavenumber Model to Modeling Radiative Transfer in a Mixture of Real Gas Media", *JQSRT*, 109, pp. 2078-2093.
- Smith, T. F., Shen, Z. F., Friedman, J. N., 1982, "Evaluation of Coefficients for the Weighted Sum of Gray Gases Model", *J. Heat Transfer*, 104, pp.602-608.
- Smith, T. F., Al-Turki, A. M., Byun, K. H., Kim, T. K., 1987, "Radiative and Conductive Transfer for a Gas/Soot Mixture Between Diffuse Parallel Plates", *J. Thermophys. Heat Transfer*, 1, pp.50-55.
- Solovjov, V. P., Webb, B. W., 2000, "SLW Modeling of Radiative Transfer in Multicomponent Gas Mixtures", *JQSRT*, 65, pp. 655-672.
- Solovjov, V. P., Webb, B. W., 2002, "A Local Spectrum Correlated Model for Radiative Transfer in Non-uniform Gas Media", *JQSRT*, 73, pp. 361-373.
- Solovjov V. P., Webb, B. W., 2010, "Application of CW Local Correction Approach to SLW Modeling of Radiative Transfer in Non-Isothermal Gaseous Media. *JQSRT*, in press.
- Texas Advanced Computing Center (TACC) <<http://services.tacc.utexas.edu/index.php/lonestar-user-guide>>

7. RESPONSIBILITY NOTICE

The authors are the only responsible for the printed material included in this paper.